This article has been accepted for publication in a future issue of this journal, but has not been fully edited. Content may change prior to final publication.
DOI: 10.17775/CSEEJPES.2025.05740

A Learning-to-Optimize Framework for Joint Scheduling in Electricity and Gas Systems

Chloé Dupont, François Vallée, *Member, IEEE,*, Bruno Francois, *Senior Member, IEEE,* and Jean-François Toubeau, *Member, IEEE,*

***Abstract*—The increasing penetration of renewable energy introduces variability and uncertainties in power systems. These challenges can be mitigated through the coordinated operation of gas and electricity resources, leveraging the flexibility of gas-fired power plants and the inherent storage capacity of gas pipelines. A key difficulty of this approach lies in accurately modeling gas flow dynamics that are typically represented by the non-convex Weymouth equation. To address this, the paper presents a two-stage Learning-to-Optimize (L2O) framework that bypasses the complexity of explicit gas flow modeling, enabling fast and reliable solutions for the coordinated day-ahead power and gas dispatch problem. The proposed L2O process uses advanced recurrent neural network architectures to forecast the next-day operational states of the gas system based on historical system data. Then, the predicted operating points are used to linearize the Weymouth equation, allowing the resulting linear constraints to be embedded into the optimization problem for improved tractability. We finally introduce a trust region to constrain solutions within a physically valid neighborhood of the predicted state. Numerical results demonstrate that our L2O approach achieves cost efficiency comparable to state-of-the-art formulations, while significantly reducing computation time.**

***Index Terms*—Encoder-decoder neural networks, Multi energy systems flexibility, Linepack, Power and gas dispatch, Weymouth equation linearization**

I. Introduction

THE increasing share of renewable energy introduces variability and uncertainty into power systems, complicating their reliable and cost-effective operation. To support a smooth transition towards a low-carbon future, Natural Gas-Fired Power Plants (NGFPPs) serve as key flexible assets, capable of rapidly adjusting their output power to balance fluctuations in supply and demand [1]. However, the strong coupling between electricity and gas networks requires coordinated operational planning; otherwise, technical limits in gas pipelines or shortages in natural gas supply can force costly redispatches and lead to inefficient resource use. Currently, both systems are operated independently, such that technical restrictions on the operation of gas networks and natural gas availability can negatively affect the dispatch of electrical systems [2], [3]. Meanwhile, the emergence of power-to-gas technologies, which convert electricity into synthetic hydrogen or methane, offers new opportunities to strengthen system flexibility by exploiting gas storage solutions, either in pipelines (through linepack flexibility [4], [5]), or via gas reservoirs [6].

A key challenge in coordinating electricity and gas systems lies in accurately modeling natural gas flow dynamics, which is essential for their effective integration into model-based optimization frameworks. Specifically, the relationship between gas pressures and flow along pipelines is governed by a set of Partial Differential Equations (PDEs) that are dependent on both time and space [7]. Although local optimization methods have been proposed to solve this problem, they are computationally demanding and thus poorly suited for operational deployment in large-scale systems [8], [9], [10].

By neglecting the inertia term, whose impact on pressure drop is small (less than 1%) [11], the gas flow PDEs are simplified into the algebraic, non-convex Weymouth equation, which captures friction-induced pressure drop via a quadratic relationship between flow and the difference of squared nodal pressures. To improve tractability of the optimization problem, various convexification techniques, mainly based on relaxations or approximations, have been proposed in the literature.

A Second-Order Cone (SOC) relaxation of the Weymouth equation is introduced in [7], by converting the original equality constraint into a convex inequality. While simplifying the problem, this relaxation admits anywhere within the interior of the quadratic cone, rather than restricting them to the boundary where physical flows occur. As a result, it can lead to significant deviations from the true gas dynamics. To mitigate this problem, [12] introduces linear approximations of the concave part, while [13] incorporates McCormick envelopes to strengthen the SOC relaxation. Further tightening is achieved in [14] through an online iterative algorithm that refines McCormick bounds around the operating point, at the expense of increased computational cost. In general, all these SOC-based relaxation are not sufficiently tight to guarantee practical accuracy within short computation times [11].

Alternative strategies rely on formulating the Weymouth equation using Piecewise Linear Approximations (PLA) [15]. Among these, the incremental approach developed in [16] has demonstrated superior performance in comparative studies [17]. The accuracy of these methods is closely related to the number of segments used to represent the gas flow equations, introducing a trade-off between computational complexity and

Manuscript received July 4, 2025; revised September 24, 2025; accepted October 29, 2025. Date of online publication xxx.

This research was carried out in the context of the Energy Transition Fund, REINVENT project, supported by the FPS Economy, SMEs, Self-Employed and Energy, Belgium.

C. Dupont (corresponding author, email : chloe.dupont@umons.ac.be), F. Vallée and J-F. Toubeau are with the Power Systems and Markets Research Group, University of Mons, Mons, Belgium

C. Dupont and B. Francois are with Univ. Lille, Arts et Metiers Institute of Technology, Centrale Lille, Junia, ULR 2697 - L2EP, F-59000 Lille, France

approximation quality [18]. An alternative in [19] linearizes the non-convex equation using Taylor expansions around fixed pressure points, yielding a set of linear upper bounds. However, by replacing the equality with inequalities, this approach enlarges the feasible set.

In general, all these convexification methods still face challenges regarding solution accuracy and computational tractability. A promising solution is the integration of Machine Learning (ML) into optimization models, offering significant performance and scalability benefits [20], [21]. For instance, authors in [22] leverage graph neural networks to estimate the calorific capacity of gas within pipeline segments, thereby reducing the need for extensive sensor deployment. In [23], neural networks replace Monte Carlo simulations in the reliability assessment of corroding natural gas pipelines. However, a notable drawback of this approach is its black-box nature, which limits interpretability and transparency in decision-making processes. In [24], the authors incorporate an input convex neural network within the optimization constraints to enforce gas flow physics. Although this approach improves modeling accuracy, it adds significant computational overhead.

In this paper, rather than modeling the full complexity of gas flows within pipelines, we focus on accurately representing the expected operating region that is most relevant for scheduling decisions. This is achieved by developing a two-stage Learning-to-Optimize (L2O) framework. In the first stage, an advanced recurrent neural network, trained offline on a dedicated database, predicts the expected optimal operating point of the gas system, explicitly capturing its complex interdependence with the electricity grid. In the second stage, the optimization problem is locally linearized around this predicted state, enabling efficient and tractable decision-making. Unlike black-box ML models that aim to directly predict the optimal decision without any guarantee on the feasibility of system constraints, our approach maintains physical interpretability and allows the optimization model to refine decisions near the predicted state. To improve the feasibility of the approach, we introduce a trust region constraint that restricts the optimization search space to a neighborhood around the predicted state. This significantly enhances solution robustness by reducing discrepancies between day-ahead scheduling and the actual real-time dispatch decisions.

The key contributions of this paper can be summarized as:

(*i*) We develop a novel Learning-to-Optimize (L2O) framework in which predicted operating points are embedded into a coordinated day-ahead electricity and gas dispatch optimization problem. To ensure computational scalability for large-scale energy systems and long planning horizons, we employ a tractable linearization of the Weymouth equation around these predicted points.

(*ii*) We introduce a trust region that ensures consistency with the physical gas flows defined by the Weymouth equation. Specifically, the equation defines a physically valid operating region, constraining the optimization to remain within a neighborhood of the predicted point. By improving solution feasibility, the approach enables to improve the ex-post performance by avoiding costly real-time redispatch actions.

(*iii*) We rely on advanced recurrent neural network architectures to predict operating points based on historical system states. This design enables the model to capture temporal dependencies and dynamic patterns in the energy systems, enhancing the accuracy and reliability of the predicted points used in the optimization process.

We demonstrate the effectiveness of our L2O approach on a realistic case study involving coupled electricity and gas systems. Results show that our method achieves modeling accuracy comparable to state-of-the-art formulations, while requiring significantly less computation time. Data and code are openly available on the following GitHub repository [25].

The remainder of this paper is organized as follows. Section II introduces the joint scheduling framework and outlines the main modeling assumptions. Section III presents the proposed L2O methodology, including the neural network predictor and the linearization scheme. Section IV details the case study, numerical setup, and results, with sensitivity analyses to assess scalability and robustness. Section V concludes the paper with perspectives for future work.

II. A COORDINATED POWER AND GAS DISPATCH

We develop a multi-energy system model integrating both electrical and gas networks within a fully coordinated framework. The joint day-ahead dispatch problem is formulated under the assumption of a single system operator, aiming to minimize total costs of power generation and gas in-feeds. The formulation enforces all operational constraints of both networks, assumes a predefined unit commitment, and treats exogenous inputs such as renewable generation and loads deterministically. Both systems are modeled with hourly time resolution.

A. Power Network Constraints

The electrical network is represented by a set of high-voltage transmission lines $(i,j) \in \mathcal{L}$ and busses $i \in \mathcal{I}$ connecting conventional power generation units $e \in \mathcal{E}$ and wind farms $w \in \mathcal{W}$ to electrical demands $d \in \mathcal{D}$. The following set of constraints ensures the safe operation of the electrical power network for each time step $t \in \mathcal{T}$:

$$\underline{P}_e \leq p_{e,t} \leq \overline{P}_e, \quad \forall e \in \mathcal{E}, \tag{1a}$$

$$f_{i,j,t} = B_{i,j}(\theta_{i,t} - \theta_{j,t}), \quad \forall (i,j) \in \mathcal{L}, \tag{1b}$$

$$-F^{\max}_{i,j} \leq f_{i,j,t} \leq F^{\max}_{i,j}, \quad \forall (i,j) \in \mathcal{L}, \tag{1c}$$

$$-\pi \leq \theta_{i,t} \leq \pi, \ \theta_{\text{ref},t} = 0, \quad \forall i \in \mathcal{I}, \tag{1d}$$

$$\sum_{e \in \mathcal{A}^{\mathcal{E}}_i} p_{e,t} + \sum_{w \in \mathcal{A}^{\mathcal{W}}_i} p_{w,t} - \sum_{(i,j) \in \mathcal{L}} f_{i,j,t} = \sum_{d \in \mathcal{A}^{\mathcal{D}}_i} p_{d,t}, \forall i \in \mathcal{I}. \tag{1e}$$

The power produced by each conventional power plant $p_{e,t}$ is bounded by its operating limits $\underline{P}_e$ and $\overline{P}_e$ (1a). Constraint (1b) defines power flows along transmission lines $f_{i,j,t}$ using the voltage angles $\theta_{i,t}$ and susceptance of the line $B_{i,j}$, while (1c) enforces the transmission capacity limits $F^{\max}_{i,j}$. Voltage angles are constrained in (1d), with the reference node angle fixed at zero. Constraint (1e) ensures nodal power balance by matching the total power injected into each bus, comprising generation from conventional units $p_{e,t}$ and wind farms $p_{w,t}$,

with the sum of power flows $f_{i,j,t}$ and local demands $p_{d,t}$. The sets $\mathcal{A}_i^{\mathcal{E}}$, $\mathcal{A}_i^{\mathcal{W}}$ and $\mathcal{A}_i^{\mathcal{D}}$ denote, respectively, the power generators, renewable units, and demand nodes connected to bus i.

B. Gas Network Constraints

The gas network is defined by a set of high-pressure nodes $m \in \mathcal{M}$ and by the pipelines $(m,n) \in \mathcal{Z}$ connecting them. Compressors are also represented through their inlet and outlet nodes $(m,n) \in \mathcal{C}$. To ensure an efficient flow of natural gas from suppliers $g \in \mathcal{G}$ to consumers $b \in \mathcal{B}$, network operations must adhere to a set of constraints :

$$\underline{P}_g \leq p_{g,t} \leq \overline{P}_g, \quad \forall g \in \mathcal{G},\ t \in \mathcal{T}, \tag{2a}$$

$$\underline{\mathrm{PR}}_m \leq pr_{m,t} \leq \overline{\mathrm{PR}}_m, \quad \forall m \in \mathcal{M},\ t \in \mathcal{T}, \tag{2b}$$

$$pr_{m,t} \leq pr_{n,t} \leq \Gamma_{m,n}\ pr_{m,t}, \quad \forall (m,n) \in \mathcal{C},\ t \in \mathcal{T}, \tag{2c}$$

$$q^2_{m,n,t} = K^2_{m,n}\left(pr^2_{m,t} - pr^2_{n,t}\right), \forall (m,n) \in \mathcal{Z}, t \in \mathcal{T}, \tag{2d}$$

$$q_{m,n,t} = \frac{q^{\text{in}}_{m,n,t} + q^{\text{out}}_{m,n,t}}{2}, \quad \forall (m,n) \in \mathcal{Z},\ t \in \mathcal{T}, \tag{2e}$$

$$h_{m,n,t} = S_{m,n}\frac{pr_{m,t} + pr_{n,t}}{2}, \quad \forall (m,n) \in \mathcal{Z},\ t \in \mathcal{T}, \tag{2f}$$

$$h_{m,n,t} = H^0_{m,n} + q^{\text{in}}_{m,n,t} - q^{\text{out}}_{m,n,t}, \forall (m,n) \in \mathcal{Z}, t = 1, \tag{2g}$$

$$h_{m,n,t} = h_{m,n,t-1} + q^{\text{in}}_{m,n,t} - q^{\text{out}}_{m,n,t}, \forall (m,n) \in \mathcal{Z}, t \in \mathcal{T}, t \neq 1 \tag{2h}$$

First, the natural gas in-feeds $p_{g,t}$ are restricted by the suppliers' operating limits $\underline{P}_g$ and $\overline{P}_g$ (2a). Then, the pressure of each node $pr_{m,t}$ is maintained between security thresholds $\underline{\mathrm{PR}}_m$ and $\overline{\mathrm{PR}}_m$ (2b). Constraint (2c) defines the operation of compressors operation, increasing gas pressure from node m to node n within the compression factor limit $\Gamma_{m,n}$. In the context of this study, only unilateral flows are considered. The equality constraint (2d) corresponds to the Weymouth equation, connecting the gas flow in a pipeline $q_{m,n,t}$ to the pressures of the corresponding inlet $pr_{m,t}$ and outlet $pr_{n,t}$ nodes. The pressure drop along the pipeline due to friction is quantified as the nodal pressure difference scaled by the known Weymouth constant $K^2_{m,n}$, which depends on temperature, gas composition, the pipeline geometry, and its friction coefficient. Constraint (2e) specifies that the physical flow $q_{m,n,t}$ is calculated as the average of the flows entering $q^{\text{in}}_{m,n,t}$ and exiting $q^{\text{out}}_{m,n,t}$ each pipeline. The last set of constraints (2f)-(2h) aims at introducing linepack flexibility to the problem, i.e., the ability to store gas $h_{m,n,t}$ within a pipeline. It is influenced by the pressure at the inlet $pr_{m,t}$ and outlet $pr_{n,t}$ nodes, and by the pipeline constant $S_{m,n}$, which is determined by physical characteristics such as diameter, length, and friction coefficient (2f). The conservation of mass principle is expressed through (2g) and (2h). The linepack is initialized with $H^0_{m,n}$ in (2g). Then, at each time step t, the linepack $h_{m,n,t}$ is updated based on the stored amount from the previous period $h_{m,n,t-1}$ and the net gas flow, i.e., the difference between injections $q^{\text{in}}_{m,n,t}$ and extractions $q^{\text{out}}_{m,n,t}$ (2h).

C. Coupling Constraint

The power and gas systems are interconnected through the operation of GFPPs, which use natural gas as a fuel source to generate electricity. This is expressed with a nodal gas balance equation for each node $m \in \mathcal{M}$ and time step $t \in \mathcal{T}$:

$$\sum_{g \in \mathcal{A}^{\mathcal{G}}_m} p_{g,t} = \sum_{e \in \mathcal{A}^{\mathcal{E}}_m} \frac{p_{e,t}}{\eta_e \cdot \nu} + \sum_{b \in \mathcal{A}^{\mathcal{B}}_m} p_{b,t} + \sum_{\substack{m:(m,n) \\ \in \mathcal{Z}}} (q^{\text{in}}_{m,n,t} - q^{\text{out}}_{m,n,t}). \tag{3}$$

Constraint (3) ensures energy conservation within the gas network at each node m. The sets $\mathcal{A}^{\mathcal{G}}_m$ and $\mathcal{A}^{\mathcal{E}}_m$ enlist the gas supply stations g and the GFPPs e connected to node m. The left-hand side of the equation therefore represents the quantity of gas injected into this node m by a supplier. The efficiency η_e of GFPPs and the conversion factor ν are used to determine the volume of gas that the facility uses to produce the electrical power $p_{e,t}$. Then, the total natural gas demand is computed as the sum of the demands $p_{b,t}$ from all consumers connected to the corresponding gas node m, defined by the set $\mathcal{A}^{\mathcal{B}}_m$. Finally, the last term expresses the inlet $q^{\text{in}}_{m,n,t}$ and outlet $q^{\text{out}}_{m,n,t}$ flows of each pipeline, which may differ due to the inclusion of linepack effects (i.e., storage of gas within the pipeline).

D. Resulting Model

The formulated coordinated day-ahead power and gas dispatch problem is expressed as :

$$\min_{\Theta} \sum_{t \in \mathcal{T}} \left(\sum_{e \in \mathcal{E}} C_e\ p_{e,t} + \sum_{g \in \mathcal{G}} C_g\ p_{g,t}\ \nu \right), \tag{4a}$$

$$\text{s.t. Electrical Network Constraints (1a)-(1e)}, \tag{4b}$$

$$\text{Gas Network Constraints (2a)-(2h)}, \tag{4c}$$

$$\text{Coupling Constraint (3)}, \tag{4d}$$

where $\Theta = \{p_{e,t}, f_{i,j,t}, \theta_{i,t}, p_{g,t}, pr_{m,t}, q_{m,n,t}, q^{\text{in}}_{m,n,t}, q^{\text{out}}_{m,n,t}, h_{m,n,t}\}$ is the set of decision variables, while C_e and C_g respectively represent the marginal generation costs of electricity for each conventional facility $e \in \mathcal{E}$ and the natural gas supply cost for each source $g \in \mathcal{G}$ (€/MWh). The conversion factor ν transforms the gas volumetric measure into its energy equivalent. By solving problem (4), the system operator seeks to minimize the total day-ahead scheduling cost of electrical power and natural gas in-feeds while ensuring compliance with the operational constraints of both systems. A key challenge in this optimization arises from the Weymouth equation (2d), a non-convex quadratic constraint that significantly increases the computational complexity of the problem. The following Section introduces our L2O framework, which was developed to address this challenge by reformulating the constraint in a more tractable manner.

III. Learning-to-Optimize (L2O) Methodology

Fig. 1 displays the L2O methodology developed in this paper. First, we predict the expected optimal operational state of the gas system (which depends on decision variables such as nodal pressure, gas flows, linepack level) for the next day using the relevant available information. Here, we use the past demands from residential, and industrial sectors, as well as the past renewable production, directly related to the

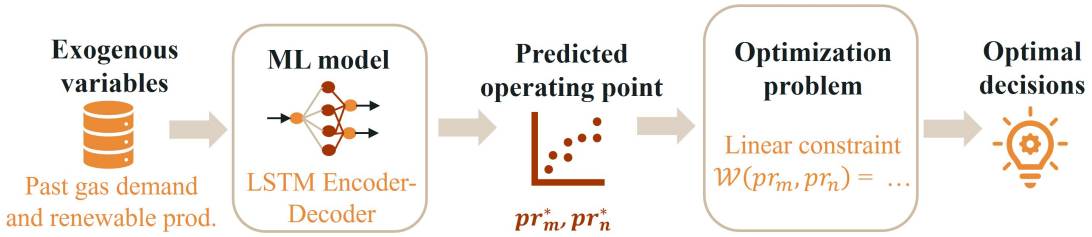

Fig. 1: Workflow diagram of the proposed L2O approach, leading to a tractable model for integrated electricity–gas scheduling.

consumption of gas-fired power plants. Specifically, we train a ML model mapping these past exogenous variables x_t to determine future operating points in terms of pressure for the gas network (pr_m^*, pr_n^*) at each time strep. Advanced recurrent neural networks are trained offline using a dedicated database, in a procedure that is further presented in subsection III-A. Second, the predicted optimal pressure levels are exploited in the downstream optimization model to capture the complex constraints governing gas flow physics. As explained in subsection III-B, the Weymouth equation is linearized around these operating points for each time step and pipeline. The resulting optimization model, which yields dispatch decisions for the multi-energy system, has a low computational cost and competitive modeling accuracy.

A. Operating Point Prediction

Predicting the behavior of gas systems presents several challenges. One major issue consists of capturing the dynamics of the state variables in the gas system, which fluctuate over time and exhibit complex patterns [26]. Here, Recurrent Neural Networks (RNNs) are therefore used for their ability to effectively model time dependencies by capturing and transmitting essential information from past inputs over time. The key characteristic of RNNs is the hidden state, which holds relevant information from past time steps, enabling the RNN to exhibit a form of memory. In particular, Long Short-Term Memory (LSTM) networks, special variants of RNNs, were developed to tackle vanishing gradient problems by regulating the flow of information propagated through time [27]. LSTMs are therefore well-suited for time-series forecasting, where past context plays a crucial role in predicting future outcomes [28].

However, in its traditional form, the LSTM model struggles with multi-time-step forecasting due to a mismatch in input dimensionality, i.e., past time steps often include realized exogenous variables that are not available for future predictions, complicating the modeling task and potentially degrading forecast accuracy. Building upon the LSTM model, the encoder–decoder architecture has become a fundamental framework in deep learning, particularly effective for sequence-to-sequence (seq2seq) tasks [29]. As represented in Fig. 2, the architecture is structured around two core modules: an encoder and a decoder, each implemented using a RNN (often based on LSTM cells).

Overall, the output sequence is predicted as follows:

$$z_K = f_{LSTM}^{enco}(x_K, z_{K-1}) \tag{5a}$$
$$\alpha_1 = f_{LSTM}^{deco}(z_K) \tag{5b}$$
$$\alpha_t = f_{LSTM}^{deco}(\alpha_{t-1}), \forall t \in \mathcal{T}, t \neq 1 \tag{5c}$$
$$y_t = a\ (\alpha_t), \forall t \in \mathcal{T} \tag{5d}$$

First, the encoder f_{LSTM}^{enco} processes the nonlinear patterns from historical input time series $x_k = (x_1, x_2, ..., x_K)$, and generates hidden states z_k at each time step using the input x_k and past hidden states z_{k-1}. The final hidden state z_K is the context vector that is trained to encompass all relevant information from the entire input sequence. The decoder f_{LSTM}^{deco} then processes z_K to generate new hidden states α_t. The final output sequence $y_t = (y_1, y_2, ..., y_T)$ of length $|\mathcal{T}|$ is obtained by applying a linear transformation a of the decoder output sequence. The architecture accommodates variable-length input and output sequences, learning the underlying mapping autonomously from the data. In contrast to classical RNNs, the encoder–decoder framework supports the integration of static variables and enables an effective temporal representation by encoding entire input sequences before generating outputs. In our L2O process, a LSTM-based encoder-decoder is thus used to predict future operating states. This architecture is specifically designed to capture both the temporal dependencies and spatial interactions that characterize coupled electricity–gas systems.

In this study, the input features x_t consist of the relevant available exogenous variables, specifically past gas demand profiles and renewable electricity generation, which have a direct impact on the gas network's operating state. Using these features, the predictor forecasts the nodal pressures (pr_m^*, pr_n^*) for the following day, providing an approximation of the system's operating point to guide the downstream optimization process.

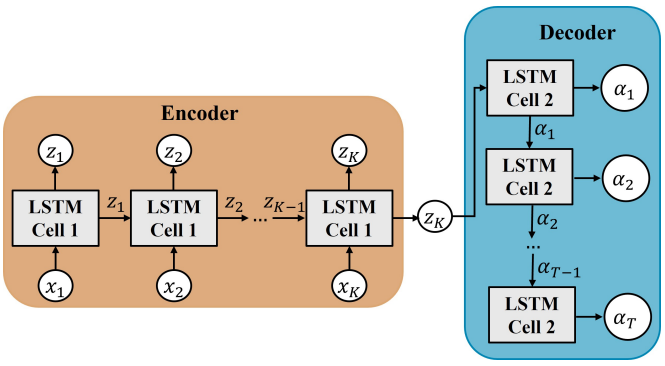

Fig. 2: LSTM encoder-decoder architecture used for time series prediction.

B. Weymouth Constraint Linearization

Once the predicted operational points (pr_m^*, pr_n^*) over the next-day scheduling horizon are available, they are leveraged to guide the optimization model by reformulating the Weymouth equation through a linear equality constraint. The original nonlinear Weymouth constraint involves two types of decision variables, i.e., pressure levels and gas flows. The LSTM encoder-decoder architecture is employed to forecast pressure levels (pr_m^*, pr_n^*) at the inlet and outlet node of each pipeline for every hour of the upcoming day. Based on this information, the Weymouth equation can be approximated locally using a first-order Taylor series expansion to derive the corresponding gas flows $q_{m,n}$. This process is represented in Fig. 3. The Weymouth constraint (2d) is thus simplified into a linear form that is computationally tractable. For conciseness, time indices are omitted and the Weymouth equation is denoted as $\mathcal{W}(pr_m, pr_n) = q_{m,n} = K_{m,n}\sqrt{(pr_m^2 - pr_n^2)}$:

$$q_{m,n} \approx \mathcal{W}(pr_m^*, pr_n^*) + \left.\frac{\partial \mathcal{W}}{\partial pr_m}\right|_{pr_m^*, pr_n^*} \cdot (pr_m - pr_m^*) + \left.\frac{\partial \mathcal{W}}{\partial pr_n}\right|_{pr_m^*, pr_n^*} \cdot (pr_n - pr_n^*), \tag{6a}$$

with:

$$\left.\frac{\partial \mathcal{W}}{\partial pr_m}\right|_{pr_m^*, pr_n^*} = K_{m,n} \frac{pr_m^*}{\sqrt{pr_m^{*2} - pr_n^{*2}}}, \tag{6b}$$

$$\left.\frac{\partial \mathcal{W}}{\partial pr_n}\right|_{pr_m^*, pr_n^*} = K_{m,n} \frac{-pr_n^*}{\sqrt{pr_m^{*2} - pr_n^{*2}}}. \tag{6c}$$

A key advantage of the proposed framework is its simplicity and computational efficiency, which make it naturally adaptable to a wide range of optimization settings where uncertainty and system complexity need to be addressed.

C. Trust Region

To improve the feasibility of the linearization (i.e., to preserve the compliance with the true underlying physical behavior of the system), a trust region is defined around the predicted point. This region allows to limit the permissible deviation of the decision variables to a neighborhood within which the linear approximation is considered valid. Practically, a new equation is added for each time step $t \in \mathcal{T}$ to the previous set of constraints (6), replacing the Weymouth equation (2d) :

$$\left| q_{m,n} - \sqrt{K_{m,n}^2 (pr_m^{*2} - pr_n^{*2})} \right| \leq \epsilon_{m,n}, \forall (m,n) \in \mathcal{Z} \tag{7}$$

where $\epsilon_{m,n}$ denotes the maximum permissible deviation between the gas flow obtained from the linearized model and the reference flow calculated at the predicted operating point (pr_m^*, pr_n^*). This additional constraint prevents the decision variable $q_{m,n}$ from deviating from the physics of the Weymouth equation (2d). In order to identify a balance between feasibility and optimality, the size of the trust region $\epsilon_{m,n}$ is here implemented as a decision variable of the optimization problem. Since smaller values of $\epsilon_{m,n}$ enforce closer adherence to the original physical relationships, $\epsilon_{m,n}$ is included in the objective function and minimized alongside the original cost in (4a), which then becomes:

$$\min_{\Theta} \sum_{t \in \mathcal{T}} \left(\sum_{e \in \mathcal{E}} C_e \; p_{e,t} + \sum_{g \in \mathcal{G}} C_g \; p_{g,t} \; \nu + \mu \sum_{(m,n) \in \mathcal{Z}} \epsilon_{m,n} \right) \tag{8}$$

where μ is a weighting coefficient, arbitrarily defined to balance the trade-off between minimizing operational costs and enforcing adherence to physical relationships.

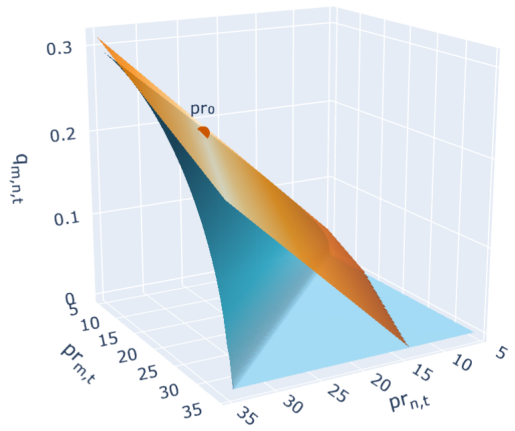

Fig. 3: Representation of the Weymouth equation for positive flows (blue) and a first order Taylor series expansion around a predicted operating point pr_0 (orange).

IV. Numerical Experiments

Numerical experiments are performed on a representative integrated energy system, combining the IEEE 14-bus power network with a 12-node natural gas grid. The test system is illustrated in Fig. 4, where Gas-Fired Power Plants (GFPPs) connect buses 3, 6, and 8 of the electrical grid to gas nodes 7, 10, and 12. In addition, two wind farms are integrated into the IEEE 14-bus system, while the generators at buses 1 and 2 are nuclear power plants. Our L2O framework, formulated as a linear problem, is evaluated against two state-of-the-art methods, further detailed in subsection IV-B: an incremental piecewise linear approximation (cast as a mixed-integer linear problem) and a second-order cone relaxation. All models are implemented in Python and solved using Gurobi 11.0.2 on an Intel CoreTM i7-13700HX processor (2.1 GHz) with 32 GB of RAM. For transparency and reproducibility, all datasets and code are made publicly available through a dedicated GitHub repository [25].

A. Data generation

The proposed L2O approach relies on constraint linearization around predicted operating points, which requires prior training of our LSTM-based encoder-decoder model. Without publicly available datasets linking gas flows and pressures to exogenous variables, a synthetic database is generated using an optimization model based on the PLA approximation. This method can accurately replicate the gas flow dynamics when sufficient breakpoints are used. Although this increases the

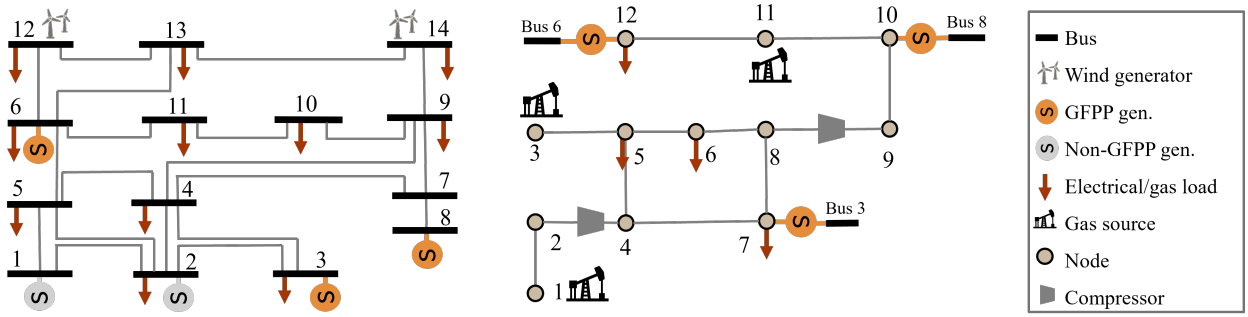

Fig. 4: Case study composed of the IEEE 14-bus system and 12-node natural gas system.

computational effort during database generation, it has no impact on the efficiency of the proposed model since this step is performed offline. While real operational data capture the true physics of the system, they are also shaped by operator practices, i.e., often heuristic and not necessarily optimal, which risks embedding biases into the predictor. By contrast, our synthetic database is derived from optimal joint dispatch solutions of the coupled electricity–gas system, ensuring training data that are both physically consistent and economically efficient, and fully aligned with the coordination objective of our study. The exogenous variables are based on Belgian hourly data from 2024, extracted from the electricity and gas transparency platforms from system operators [30], [31]. The optimization problem is therefore executed over a year, with renewable electricity production and gas consumption varying throughout this period. The hourly decision variables regarding gas network operation are collected to build the database. We then use 80% of this dataset to train the predictor, i.e., our encoder-decoder architecture learns the complex mapping from external conditions to gas network operating points. The remaining 20% of the data is evenly split between a validation set, used for hyperparameter tuning, and a test set for final performance evaluation.

B. Benchmarks

We present two alternative formulations of the Weymouth equation, which serve as benchmarks for the numerical experiments. We compare our complete L2O framework against these two state-of-the-art convexification techniques: the incremental piecewise linear approximation and the second-order cone relaxation enriched with McCormick envelopes.

1) Incremental piecewise linear approximation: A first approach to approximate the Weymouth equation involves using piecewise linear functions. In particular, the incremental method described in [16] has demonstrated superior performance to other piecewise linear models for the representation of gas networks [17]. By introducing auxiliary variables, this method linearizes the quadratic terms of the Weymouth equation, $q^2_{m,n,t}$ and $pr^2_{m,t}$. Practically, a set of breakpoints is established over the flow and pressure domains, and linear interpolation is performed between these points. Therefore, a set of additional constraints needs to be incorporated into the initial model along with binary variables to ensure the formulation consistency. This method entails a trade-off between approximation accuracy and computational complexity. Increasing the number of breakpoints enhances the fidelity of the gas flow and pressure representation. However, it also leads to a larger number of binary variables and additional constraints, thereby increasing the computational burden of the resulting optimization problem.

2) Second-order cone relaxation: A second widely adopted approach to handle the non-convexity of the Weymouth equation is to apply a relaxation technique. The original equality (2d) can be decomposed into :

$$q^2_{m,n,t} \leq K^2_{m,n}\ (pr^2_{m,t} - pr^2_{n,t}),\ \forall (m,n) \in \mathcal{Z}, t \in \mathcal{T} \quad \text{(9a)}$$
$$q^2_{m,n,t} \geq K^2_{m,n}\ (pr^2_{m,t} - pr^2_{n,t}),\ \forall (m,n) \in \mathcal{Z}, t \in \mathcal{T} \quad \text{(9b)}$$

The non-convex equality is relaxed by omitting the lower bound (9b), and retaining only the second-order cone (SOC) constraint (9a). Yet, the resulting convex formulation expands the feasible set to include solutions that may not adhere to the physical constraints of gas flow, i.e., solutions outside the feasible region defined by the original Weymouth equation, as illustrated by the area under the blue curve in Fig. 3. To mitigate modeling inaccuracies, authors in [13] tighten the relaxation through the incorporation of McCormick envelopes. In our framework, we adopt the same approach, introducing additional constraints and auxiliary variables to restrict the feasible region and exclude non-physical operating points. This requires predefined bounds on gas flows as well as on the sum and difference of nodal pressure levels, parameters that are often nontrivial to estimate accurately.

C. Analysis of results

We perform a feasibility assessment of the solutions generated by our L2O approach, benchmarked against an incremental piecewise linear approximation and an established SOC-based relaxation. Specifically, we solve the joint electricity and gas dispatch problem using: (i) the proposed L2O framework, based on different architectures for the predictor (i.e., a classical MLP, a LSTM network and the proposed encoder-decoder structure) ; (ii) the incremental piecewise linear model, evaluated with 5 and 10 breakpoints; and (iii) one SOC-based convex relaxation method using McCormick envelopes. Then, we extract two decision variables, namely, the gas flows $q_{m,n,t}$ and nodal pressures $pr_{m,t}$, from each

TABLE I: Comparison of the L2O approach and other Weymouth approximation techniques

	Enco-Deco L2O		**Single LSTM L2O**		**MLP L2O**		**PLA**		**SOCP**
	No ϵ	Ideal ϵ	No ϵ	Ideal ϵ	No ϵ	Ideal ϵ	10 BP	20 BP	
Rel MAE [%]	5.07	0.77	5.16	5.98	11.64	12.86	2.02	0.49	14.01
MAE [MNm^3]	0.0035	0.0005	0.0036	0.0041	0.0079	0.0083	0.0014	0.0004	0.0125
STD [MNm^3]	0.0073	0.0009	0.0086	0.008	0.0162	0.0150	0.0017	0.0005	0.0092
Time [s]	3	4	3	4	3	4	36	300	3

model. To evaluate the fidelity of the solutions with respect to the Weymouth equation (2d), we compute the absolute deviation between its left- and right-hand sides, defined as:

$$\Delta_{m,n,t} = \mid q^2_{m,n,t} - K^2_{m,n}\left(pr^2_{m,t} - pr^2_{n,t}\right) \mid, \forall (m,n) \in \mathcal{Z}, t \in \mathcal{T} \tag{10}$$

Table I presents three performance metrics calculated using the above deviation (10), i.e., (i) Mean Absolute Errors (MAE) and standard deviations (STD) averaged over all pipelines and time periods for the gas flows, (ii) a relative MAE (Rel MAE) to evaluate the error impact compared to the maximal flow in the concerned pipe, and (iii) the computational time.

Table I shows the performance metrics for each L2O method with and without considering the trust region ϵ. We observe that the best outcome is obtained for the encoder-decoder structure when the trust region is considered in the optimization model. In that case, the relative MAE is quite low, reaching 0.77%, which highlights a very precise estimation of gas flows. When the trust region is not considered, the error increases up to 5.07%, showing that the trust-region plays a crucial role in keeping the linearization confined to a physically relevant region.

The L2O method (with the trust region) using a traditional LSTM (relative MAE of 5.16%) or a MLP (relative MAE of 11.64%) as forecaster generates poor outcomes. A detailed analysis of those results indicate that, although the predicted pressure points across different pipelines over the daily horizon are close to realistic values individually, they are inconsistent regarding spatio-temporal dependencies. As a result, when such points are used as references in the optimization process, the spatial and temporal consistency of gas network physics cannot be preserved, leading to suboptimal scheduling decisions. This demonstrates the importance of properly capturing space-time dependencies, a task that our LSTM-based encoder-decoder model effectively handles [32]. In contrast, standard MLPs fail to capture temporal dynamics, while conventional LSTMs cannot manage long-term dependencies across a system of this scale.

Then, these results are compared with the Piecewise Linear Approximation (PLA). In terms of modeling accuracy, the proposed L2O approach, combining an encoder-decoder predictor with a trust region, achieves superior performance (0.77%) compared to the PLA with 10 breakpoints (2.02%) and comes close to the accuracy obtained with the PLA using 20 breakpoints (0.49%). Although increasing the number of segments of the PLA improves modeling accuracy, it also leads to a substantial rise in computation time, which escalates from 36 seconds (for 10 breakpoints) to 300 seconds (for 20 breakpoints). In contrast, a key strength of our approach is its very low computation time: on average, it requires only 3–4 seconds to obtain the next-day schedule, which is 9 to 75 times faster than the PLA with 10 and 20 breakpoints, respectively. This reduction in computation time could have a considerable impact, particularly for large-scale networks. In our approach, the Weymouth equation is substituted with a linear expression, ensuring that the computational complexity does not increase with system size. By contrast, PLA-based formulations introduce binary variables and additional constraints for each segment and pipeline, which can become highly detrimental when applied to large-scale systems [33].

Finally, the SOC relaxation tightened with McCormick envelopes displays the least accurate results with a relative MAE of 14.01%. While this method proves to be effective in certain scenarios, it is not universally applicable across all network operating conditions, as the relaxation of equation (2d) enlarges the feasible solution space to include physically inconsistent values. Moreover, McCormick envelopes are not scalable to high-dimensional gas networks or for close to real-time decision-making.

The outcomes of our L2O method can be observed for a specific day on Fig. 5, which displays relative MAEs in gas flows modeling for each time step and each pipeline of the gas network. Two main insights can be derived from these results.

First, the L2O approaches using a traditional LSTM or MLP show isolated instances of large modeling errors in Figs. (5b) and (5c). This pattern likely results from a sub-optimal choice of the predicted operating point, suggesting that LSTM and MLP architectures cannot adequately model the intricate spatial and temporal dependencies of gas flows. The errors produced by our encoder–decoder are not only smaller in magnitude but also more evenly distributed across the pipelines, which is essential for maintaining spatial and temporal consistency in scheduling.

Second, Figs. (5d) and (5e) clearly demonstrate the impact of adding breakpoints in the definition of the linear approximation. The 20-segment formulation presents low error, but requires substantial computation time. Finally, Fig. (5f) illustrates that the SOC-based relaxations lack sufficient tightness for practical implementation. Specifically, the SOC method yields the highest MAE among the compared techniques and systematically underestimates gas flows. This occurs because the relaxed feasible region lies beneath the true Weymouth curve. As a result, the optimization, which is driven by cost minimization, tends to exploit this enlarged feasible set by scheduling lower gas inflows than physically realistic for the corresponding pressure levels.

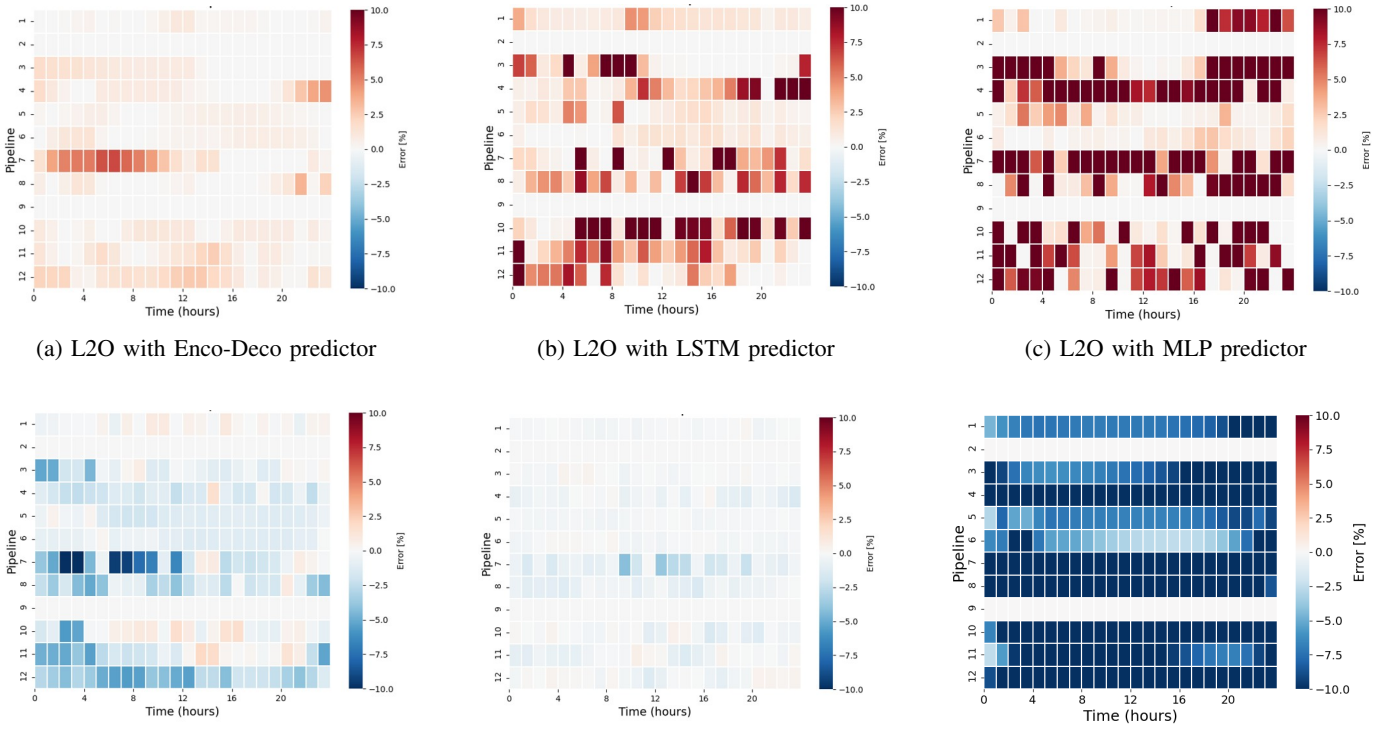

(a) L2O with Enco-Deco predictor (b) L2O with LSTM predictor (c) L2O with MLP predictor

(d) PLA with 10 breakpoints (e) PLA with 20 breakpoints (f) SOC relaxation

Fig. 5: Matrix plot of the relative MAE between right-hand and left-hand sides of relaxed/approximated Weymouth equations for each time step (x-axis) and each pipeline (y-axis)

D. Sensitivity analyses

A key contribution of this work is the integration of a trust region to limit deviations of gas flows from the predicted operating point. Incorporated into the objective function alongside dispatch costs, the weight μ in (8) assigned to this penalization term can influence the overall modeling accuracy. Fig. 6 displays the evolution of the global relative MAE depending on μ. A larger value of μ increases the emphasis on the trust region term in the objective function, thereby more strongly penalizing deviations from the predicted operating point. The lowest relative error is achieved when $\mu = 0.5$. In this case, the model retains enough flexibility to approximate the gas flow physic, avoiding over-constraining the solution, while remaining close to the predicted operating point.

As detailed in subsection III-A, several predictor architectures were evaluated for our L2O model. These predictors are

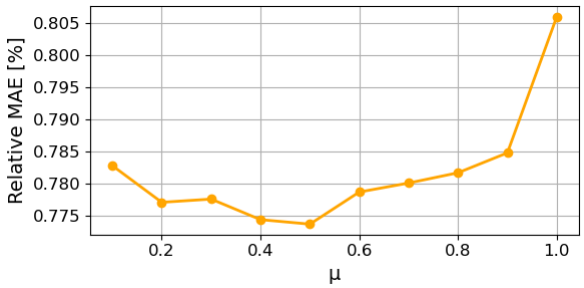

Fig. 6: Impact of μ on modeling errors

TABLE II: Comparison of the predictor performances to provide pressure operating points

	Enco-Deco	LSTM	MLP
LSTM units	12	12	0
Dense units	24	48	512+256
Rel MAE [%]	1.58	1.99	2.01
MAE [bar]	0.36	0.46	0.46
STD [bar]	0.48	0.57	0.58
Training Time [s]	130	124	14

used to determine the expected optimal operational point of the gas network at each node and time step for the upcoming day, based on gas consumption and electricity production from renewable sources over the past three days. Table II summarizes the performance of the encoder-decoder architecture, LSTM network, and MLP, after optimizing their respective hyperparameters.

A notable observation is that the MLP architecture requires significantly more units than RNNs, as it lacks an inherent mechanism for processing time-series data. Consequently, temporal features must be distributed across a larger number of parameters. Overall, the encoder-decoder architecture delivers the most accurate predictions, achieving an error rate of 1.58%, compared to 1.99% and 2.01% for the LSTM and the MLP. This superior performance stems from the model's ability to capture complex temporal patterns while simultaneously encoding spatial dependencies among nodes into a context vector that reflects the interdependencies across the network,

thereby improving the accuracy of operating state forecasts. The effectiveness of this deep learning architecture has already been demonstrated in several other domains. For instance, in large-scale flood prediction, it was applied to grids ranging from 1 to 15,000 cells while achieving optimal performance with 200 cells, thereby confirming the flexibility and scalability of the approach [34]. This improvement comes at the cost of increased training time, with the model requiring 130 seconds, compared to 124 seconds for the LSTM and 14 seconds for the MLP. However, this increase in training time is not a significant concern, as the predictor is trained only once on historical data, and it does not affect the operational efficiency (i.e., runtime performance) of the downstream optimization. Furthermore, the small prediction errors observed have only a minor impact on scheduling performance, as the optimization stage naturally readjusts dispatch decisions to preserve feasibility under physical and operational constraints. In effect, it serves as a corrective layer that compensates for minor inaccuracies in the predicted operating points.

To further assess the robustness of the proposed approach, we conducted an additional sensitivity analysis comparing the developed L2O method with the two benchmark formulations (PLA with 20 breakpoints and SOCP) under extreme operating conditions. As renewable generation accounts for nearly one-fourth of the power system's installed capacity, its variability has a significant impact on the overall operating state of the coupled networks. In particular, we selected days characterized by exceptionally low renewable availability (renewable capacity factor below 15%) and by exceptionally high availability (above 80%). Table III summarizes the performance of the three methods under these extreme cases.

Overall, these results confirm that the L2O method is robust to varying operating conditions, maintaining low error and stable runtimes across different system stress levels, consistent with the global mean (0.77%). In both extreme renewable scenarios, the PLA with 20 breakpoints remains the most precise approach, but this accuracy comes at the cost of a much higher computational burden compared to L2O and SOCP. The SOCP relaxation, however, exhibits a strong dependence on the stress level of the system: it performs better when the gas network is heavily loaded (low renewable production) with a modeling error of 12.08%, but loses significant accuracy (16.37%) when renewables dominate and gas demand decreases. This behavior stems from the fact that, under lighter loading conditions, the actual operating point lies deeper inside the relaxation cone of the Weymouth equation. It can be observed in Fig. 3 that, for identical pressure levels, the relaxed cone admits lower gas flows than the true nonlinear relationship, thereby increasing modeling errors.

TABLE III: Comparison of L2O approach, PLA, and SOCP performance under extreme renewable production scenarios

	L2O Ideal ϵ	**PLA** 20 BP	**SOCP**
	Renew. capacity factor $<$ 15%		
Rel MAE [%]	0.67	0.43	12.08
Time [s]	4	284	3
	Renew. capacity factor $>$ 80%		
Rel MAE [%]	0.78	0.52	16.37
Time [s]	4	352	3

V. Conclusion and Perspectives

In this paper, we address the modeling challenges associated with gas flow dynamics in the context of a coordinated power and gas dispatch problem. To this end, we propose a two-stage Learning-to-Optimize (L2O) framework, where a LSTM-based encoder-decoder predicts the expected optimal operating point, around which the optimization problem is locally linearized to enable efficient and tractable decision-making. Through numerical experiments, we demonstrate the effectiveness of our advanced prediction architecture in capturing the complex spatial and temporal dependencies in gas network variables. Our L2O method achieves comparable or even better modelling accuracy than the state-of-the-art techniques, while significantly reducing computation time. Additionally, introducing a trust region around the predicted point effectively limits deviation from true physical constraints during optimization, enhancing the feasibility of the scheduling solution.

In future research, our L2O approach could be further enhanced by training the predictor within a decision-focused learning framework that directly incorporates the outcomes of the optimization problem into the learning process. This integration would guide the forecaster to learn the dependencies most critical for scheduling optimization, thereby aligning its training objective with the quality of the final decisions and potentially improving overall system performance. Moreover, a dedicated scalability study will be conducted to further assess the performance of the proposed method on larger and more complex networks.

References

[1] P. Pinson, L. Mitridati, C. Ordoudis, and J. Østergaard, "Towards fully renewable energy systems: Experience and trends in denmark," *CSEE Journal of Power and Energy Systems 3.1*, pp. 26–35, 2017.

[2] M. Gil, P. Dueñas, and J. Reneses, "Electricity and natural gas interdependency: Comparison of two methodologies for coupling large market models within the european regulatory framework," *IEEE Transactions on Power Systems*, vol. 31, no. 1, pp. 361–369, 2016.

[3] S. Wang, H. Hui, Y. Ding, and J. Zhai, "Decentralized demand response for energy hubs in integrated electricity and gas systems considering linepack flexibility," *IEEE Internet of Things Journal*, vol. 11, no. 7, pp. 11 848–11 861, 2024.

[4] N. Keyaerts, W. D'haeseleer, and S. Proost, "Gas balancing and linepack flexibility: concepts and methodologies for organizing and regulating gas balancing in liberalized and integrated eu gas markets," Ph.D. dissertation, KU Leuven, 2012.

[5] S. Clegg and P. Mancarella, "Integrated electrical and gas network flexibility assessment in low-carbon multi-energy systems," *IEEE Transactions on Sustainable Energy*, vol. 7, no. 2, pp. 718–731, 2016.

[6] A. Belderbos, T. Valkaert, K. Bruninx, E. Delarue, and W. D'haeseleer, "Facilitating renewables and power-to-gas via integrated electrical power-gas system scheduling," *Applied Energy*, vol. 275, p. 115082, 2020.

[7] C. Borraz-Sánchez, R. Bent, S.Backhaus, H. Hijazi, and P. V. Hentenryck, "Convex relaxations for gas expansion planning," *INFORMS Journal on Computing*, vol. 28, pp. 645–656, 11 2016.

[8] A. Zlotnik, L. Roald, S. Backhaus, M. Chertkov, and G. Andersson, "Coordinated scheduling for interdependent electric power and natural gas infrastructures," *IEEE Transactions on Power Systems*, vol. 32, no. 1, pp. 600–610, 2017.

[9] C. O. Malley, G. Hug, and L. L. Roald, "Stochastic hybrid approximation for uncertainty management in gas-electric systems," *IEEE Transactions on Power Systems*, vol. 37, no. 3, pp. 2208–2219, 2022.
[10] S. R. Kazi, K. Sundar, S. Misra, S. Tokareva, and A. Zlotnik, "Intertemporal uncertainty management in gas-electric energy systems using stochastic finite volumes," *Electric Power Systems Research*, vol. 235, p. 110748, 2024.
[11] E. Raheli, Y. Werner, and J. Kazempour, "Flexibility of integrated power and gas systems: Gas flow modeling and solution choices matter," *IEEE Transactions on Power Systems*, vol. 40, no. 3, pp. 2130–2142, 2025.
[12] C. Wang, W. Wei, J. Wang, L. Bai, Y. Liang, and T. Bi, "Convex optimization based distributed optimal gas-power flow calculation," *IEEE Transactions on Sustainable Energy*, vol. 9, no. 3, pp. 1145–1156, 2018.
[13] A. Schwele, C. Ordoudis, J. Kazempour, and P. Pinson, "Coordination of power and natural gas systems: Convexification approaches for linepack modeling," *2019 IEEE Milan PowerTech*, pp. 1–6, 2019.
[14] S. Chen, A. J. Conejo, R. Sioshansi, and Z. Wei, "Unit commitment with an enhanced natural gas-flow model," *IEEE Transactions on Power Systems*, vol. 34, no. 5, pp. 3729–3738, 2019.
[15] C. Shao, X. Wang, M. Shahidehpour, X. Wang, and B. Wang, "An milp-based optimal power flow in multicarrier energy systems," *IEEE Transactions on Sustainable Energy*, vol. 8, no. 1, pp. 239–248, 2017.
[16] C. M. Correa-Posada and P. Sánchez-Martín, "Integrated power and natural gas model for energy adequacy in short-term operation," *IEEE Transactions on Power Systems*, vol. 30, no. 6, pp. 3347–3355, 2015.
[17] ——, "Gas network optimization: A comparison of piecewise linear models," [Online]. Available at https://optimization-online.org/2014/10/4580/ (01/04/2025).
[18] X. Zhang, M. Shahidehpour, A. Alabdulwahab, and A. Abusorrah, "Hourly electricity demand response in the stochastic day-ahead scheduling of coordinated electricity and natural gas networks," *IEEE Transactions on Power Systems*, vol. 31, no. 1, pp. 592–601, 2016.
[19] C. Ordoudis, S. Delikaraoglou, J. Kazempour, and P. Pinson, "Market-based coordination of integrated electricity and natural gas systems under uncertain supply," *European Journal of Operational Research*, vol. 287, no. 3, pp. 1105–1119, 2020.
[20] G. R., Z. Haiwang, Z. Guanglun, H. Yiliu, W. Xuan, and P. Tianjiao, "Review of learning-assisted power system optimization," *CSEE Journal of Power and Energy Systems*, vol. 7, no. 2, pp. 221–231, 2021.
[21] M. Khodayar, G. Liu, J. Wang, and M. E. Khodayar, "Deep learning in power systems research: A review," *CSEE Journal of Power and Energy Systems*, vol. 7, no. 2, pp. 209–220, 2021.
[22] Z. Yang, Z. Liu, J. Zhou, C. Song, Q. Xiang, Q. He, J. Hu, M. H. Faber, E. Zio, Z. Li, H. Su, and J. Zhang, "A graph neural network (gnn) method for assigning gas calorific values to natural gas pipeline networks," *Energy*, vol. 278, p. 127875, 2023.
[23] K. Wen, L. He, J. Liu, and J. Gong, "An optimization of artificial neural network modeling methodology for the reliability assessment of corroding natural gas pipelines," *Journal of Loss Prevention in the Process Industries*, vol. 60, pp. 1–8, 2019.
[24] V. Dvorkin, S. Chevalier, and S. Chatzivasileiadis, "Emission-constrained optimization of gas networks: Input-convex neural network approach," in *2023 62nd IEEE Conference on Decision and Control (CDC)*, 2023, pp. 1575–1579.
[25] C. Dupont, F. Vallée, B. Francois, and J.-F. Toubeau, "Online github : L20-gas-elec-coordination," Available at https://github.com/chloe-dpnt/L2O-gas-elec-coordination (24/06/2025).
[26] A. Arrigo, J.-F. Toubeau, I. Fattahi, Z. De Grève, and F. Vallée, "Distributionally robust power and gas dispatch with multivariate and correlated uncertainty," in *2022 17th International Conference on Probabilistic Methods Applied to Power Systems (PMAPS)*, 2022, pp. 1–6.
[27] S. Hochreiter and J. Schmidhuber, "Long short-term memory," *Neural Computation*, vol. 9, no. 8, 1997.
[28] J.-F. Toubeau, J. Bottieau, F. Vallée, and Z. De Grève, "Deep learning-based multivariate probabilistic forecasting for short-term scheduling in power markets," *IEEE Transactions on Power Systems*, vol. 34, no. 2, pp. 1203–1215, 2019.
[29] K. Cho, B. van Merrienboer, D. Bahdanau, and Y. Bengio. (2014) On the properties of neural machine translation: Encoder-decoder approaches.
[30] E. Group, "Open data elia," Available at https://opendata.elia.be/pages/home/ (02/02/2025).
[31] Fluxys, "Fluxys belgium electronic data platform," Available at https://gasdata.fluxys.com/en (02/02/2025).
[32] J.-F. Toubeau, T. Morstyn, J. Bottieau, K. Zheng, D. Apostolopoulou, Z. De Grève, Y. Wang, and F. Vallée, "Capturing spatio-temporal dependencies in the probabilistic forecasting of distribution locational marginal prices," *IEEE Transactions on Smart Grid*, vol. 12, no. 3, pp. 2663–2674, 2021.
[33] L. Yao, X. Wang, T. Ding, Y. Wang, X. Wu, and J. Liu, "Stochastic day-ahead scheduling of integrated energy distribution network with identifying redundant gas network constraints," *IEEE Transactions on Smart Grid*, vol. 10, no. 4, pp. 4309–4322, 2019.
[34] G. Wei, W. Xia, B. He, and C. Shoemaker, "Quick large-scale spatiotemporal flood inundation computation using integrated encoder-decoder lstm with time distributed spatial output models," *Journal of Hydrology*, vol. 634, p. 130993, 2024.

Chloé Dupont received the M.Sc. degree in electrical engineering from the University of Mons, Mons, Belgium, in 2023, where she is currently pursuing a Ph.D. degree in electrical engineering with the Power Systems and Markets Research Group. Her research interests include decision-making in power system operations, machine learning techniques for energy applications, and multi-energy systems coupling.

François Vallée (Member, IEEE) received the degree in civil electrical engineering and the Ph.D. degree in electrical engineering from the Faculty of Engineering, University of Mons, Belgium, in 2003 and 2009, respectively, where he is currently a Professor and the Leader of the "Power Systems and Markets Research Group." His research interests include PV and wind generation modeling for electrical system reliability studies in presence of dispersed generation. His Ph.D. work was awarded the SRBE/KBVE Robert Sinave Award in 2010.

Bruno François (Senior Member, IEEE) is a Full Professor at Centrale Lille Institute and at the Laboratory of Electrical Engineering and Power electronics (L2EP) in Lille, France. He received the Ph.D. degree in 1996, in Electrical Engineering. His research interests include the advanced energy management of power systems, adaptive and predictive control with AI technologies, coupling of energy systems and uncertainty impact in operation of electrical systems.

Jean-François Toubeau (Member, IEEE) received the degree in civil electrical engineering and the Ph.D. degree in electrical engineering from the University of Mons, Belgium, in 2013 and 2018, respectively, where he is currently a Full-Time Senior Researcher within the "Power Systems and Markets Research Group." His research mainly focuses on bridging the gap between machine learning and decision-making in modern power systems.